

# Direct observation of quark–hadron duality in the free neutron $F_2$ structure function

I. Niculescu,<sup>1</sup> G. Niculescu,<sup>1</sup> J. Arrington,<sup>2</sup> R. Ent,<sup>3</sup> K. A. Griffioen,<sup>4</sup>  
N. Kalantarians,<sup>5</sup> C. E. Keppel,<sup>3</sup> S. Kuhn,<sup>6</sup> W. Melnitchouk,<sup>3</sup> and S. Tkachenko<sup>7</sup>

<sup>1</sup>*James Madison University, Harrisonburg, Virginia 22807, USA*

<sup>2</sup>*Argonne National Laboratory, Argonne, Illinois 60439, USA*

<sup>3</sup>*Thomas Jefferson National Accelerator Facility, Newport News, Virginia 23606, USA*

<sup>4</sup>*College of William and Mary, Williamsburg, Virginia 23187, USA*

<sup>5</sup>*Hampton University, Hampton, Virginia 23668, USA*

<sup>6</sup>*Old Dominion University, Norfolk, Virginia 23529, USA*

<sup>7</sup>*University of Virginia, Charlottesville, Virginia 22901, USA*

(Dated: December 8, 2014)

Using data from the recent BONuS experiment at Jefferson Lab, which utilized a novel spectator tagging technique to extract the inclusive electron–free neutron scattering cross section, we obtain the first direct evidence for quark–hadron duality in the neutron  $F_2$  structure function. The data are used to reconstruct the lowest few ( $N = 2, 4$  and  $6$ ) moments of  $F_2$  in the three prominent nucleon resonance regions, as well as integrated over the entire resonance region. Comparison with moments computed from global parametrizations of parton distributions suggests that quark–hadron duality holds locally for the neutron in the second and third resonance regions for  $Q^2$  between 1 and  $\approx 4$  GeV<sup>2</sup>, with violations of  $\sim 20\%$  observed in the first resonance region.

## I. INTRODUCTION

Inclusive lepton scattering has for many decades been the most important tool with which to probe the internal quark and gluon (or parton) structure of nucleons and nuclei. Structure functions extracted from inclusive deep-inelastic scattering (DIS) experiments display the central features of quantum chromodynamics (QCD) — asymptotic freedom at short distances (*via* structure function scaling and its violation) and confinement at large distance scales (*via* the momentum dependence of parton distributions).

Since the late 1960s, DIS experiments have yielded an impressive data set that maps nucleon structure functions over several orders of magnitude in the Bjorken scaling variable,  $x$ , and the squared four-momentum transfer,  $Q^2$ . These data, supplemented by cross sections from hadronic collisions and other high-energy processes, have enabled a detailed picture of the parton distribution functions (PDFs) of the nucleon to emerge through global QCD analyses (see Refs. [1, 2] and references therein).

At lower energies, where nonperturbative quark–gluon interactions are important and the inclusive lepton–nucleon cross section is dominated by nucleon resonances, the structure functions reveal another intriguing feature of QCD, namely, quark–hadron duality. Here, the low energy cross section, when averaged over appropriate energy intervals, is found to resemble the high energy result, whose  $Q^2$  dependence is described by perturbative QCD. In this context, quark–hadron duality provides a unique perspective on the relationship between confinement and asymptotic freedom, and establishes a critical link between the perturbative and nonperturbative regimes of QCD.

In the framework of QCD, quark–hadron duality can be formally interpreted in terms of structure function moments [3]. From the operator product expansion (OPE),

the moments can be expressed as a series in  $1/Q^2$ , with coefficients given by matrix elements of local quark–gluon operators of a given twist [4]. The leading (twist 2) term corresponds to scattering from a single parton, while higher twist terms correspond to multi–quark and quark–gluon interactions. Since at low  $Q^2$  the resonance region makes a significant contribution to the structure function moments, one might expect a strong  $Q^2$  dependence of the low- $Q^2$  moments arising from the higher twist terms of the OPE. In practice, however, the similarity of the structure function moments at low  $Q^2$  and the moments extracted at high energies suggests the dominance of the leading twist contribution. The higher twist, multi-parton contributions appear to play a relatively minor role down to scales of the order  $Q^2 \sim 1$  GeV<sup>2</sup> or even lower.

This non-trivial relationship between the low-energy cross section and its deep-inelastic counterpart was first observed by Bloom and Gilman [5, 6] in the early DIS measurements that were instrumental in establishing structure function scaling. More recently, the availability of extensive, precise structure function data from Jefferson Lab, over a wide range of kinematics, has opened up the possibility for in-depth studies of quark–hadron duality. Duality has now been observed in the proton  $F_2$  and  $F_L$  structure functions [7–11], the  $F_2$  structure function of nuclei [12], the spin-dependent  $g_1$  structure functions of the proton and  $^3\text{He}$  [13–15], and the individual helicity-1/2 and 3/2 virtual photoproduction cross sections for the proton [16].

To establish the dynamical origin of quark–hadron duality requires also understanding the structure of the neutron. Four-quark higher twists contributions suggest that duality in the proton could arise from accidental cancellations between quark charges, which would not occur for the neutron [17]. Unfortunately, the absence of high-density free neutron targets means that essentially

all information on the structure functions of the neutron has had to be derived from measurements on deuterium. Typically, the deuterium data are corrected for Fermi smearing and other nuclear effects [18–23], which introduces an element of model dependence into the extraction procedure. This is particularly problematic in the nucleon resonance region, where Fermi motion effects leads to significant smearing of the resonant structures. The existence of duality in the neutron  $F_2$  structure function was suggested recently [18] in an analysis which used an iterative deconvolution method [24] to extract neutron resonance spectra from inclusive proton and deuteron  $F_2$  data [8]. A direct confirmation of duality in the neutron, however, was to date not possible.

Recently, a new experimental technique, based on spectator nucleon tagging [25], has been used to extract the free neutron  $F_2$  structure function [26]. By detecting low-momentum protons at backward angles in electron deuteron scattering, the BONuS experiment at Jefferson Lab measured  $F_2^n$  in both the resonance and DIS regions, with minimal uncertainty from nuclear smearing and rescattering corrections [27]. In the present work, we use the BONuS data to quantify for the first time the degree to which duality holds for the  $F_2$  structure function of the free neutron. Because the results reported here use data from an experimentally-isolated neutron target, one expects significantly reduced systematic uncertainties compared with those in the model-dependent analysis of inclusive deuterium data [18].

For the theoretical analysis of duality we use the method of “truncated” structure function moments [28–31], which were applied to the resonance region  $F_2$  proton data by Psaker *et al.* [32]. Here, the  $n$ -th truncated moment of the  $F_2$  structure function is defined as

$$M_N(x_{\min}, x_{\max}, Q^2) = \int_{x_{\min}}^{x_{\max}} dx x^{N-2} F_2(x, Q^2), \quad (1)$$

where the integration over  $x$  is restricted to an interval between  $x_{\min}$  and  $x_{\max}$ . This method avoids extrapolation of the integrand into poorly mapped kinematic regions, and is particularly suited for the study of duality where an  $x$  region can be defined by a resonance width around an invariant mass  $W^2 = M^2 + Q^2(1-x)/x$ , where  $M$  is the nucleon mass. As the position of the resonance peak varies with  $x$  for different  $Q^2$  values, the values for  $x_{\min}$  and  $x_{\max}$  evolve to the appropriate invariant mass squared region. For the BONuS data, we consider four ranges in  $W^2$ , corresponding to the three prominent resonance regions as well as the combined resonance region,

$$\begin{aligned} 1.3 \leq W^2 \leq 1.9 \text{ GeV}^2 & \quad [1\text{st (or } \Delta) \text{ region}], \\ 1.9 \leq W^2 \leq 2.5 \text{ GeV}^2 & \quad [2\text{nd region}], \\ 2.5 \leq W^2 \leq 3.1 \text{ GeV}^2 & \quad [3\text{rd region}], \\ 1.3 \leq W^2 \leq 4.0 \text{ GeV}^2 & \quad [\text{total resonance}]. \end{aligned} \quad (2)$$

After reviewing the BONuS experiment in Sec. II, the results for several low moments (corresponding to  $N = 2$ ,

4 and 6) of the neutron  $F_2$  structure function are presented in Sec. III. The implications of the new data for local quark-hadron duality and its violation are discussed by comparing with recent global PDF parametrizations and previous model-dependent data analyses (Sec. III A). The isospin dependence of local duality is studied by comparing the neutron moments with corresponding moments of the proton  $F_2$  structure function (Sec. III B). Finally, we summarize our results and conclusions in Sec. IV.

## II. THE BONuS EXPERIMENT

The results reported here rely on a novel experimental technique aimed at eliminating or substantially reducing the theoretical uncertainties involved in extracting neutron data from nuclear targets. The BONuS (Barely Off-shell Nucleon Structure) experiment at Jefferson Lab [25–27] used a Radial Time Projection Chamber (RTPC) to detect low momentum spectator protons produced in electron–deuteron scattering in conjunction with electrons detected with CLAS [33] in Hall B. By tagging backward moving protons one minimizes final state interactions [34–36], while the restriction to low momentum spectators ensures that the neutron is nearly on-shell and that Fermi smearing effects are essentially eliminated [26].

The BONuS experiment ran in 2005 and acquired electron–deuteron scattering data at two electron beam energies,  $E = 4.223$  and  $5.262$  GeV. The RTPC consisted of three layers of gas electron multipliers surrounding a thin, pressurized gas deuterium target which detected protons with momenta as low as  $70$  MeV/c. The experiment and data analysis are described in detail in Ref. [27]. Ratios of neutron to proton  $F_2$  structure functions and the absolute neutron  $F_2$  structure function were extracted over a wide kinematic range and for spectator proton momenta between  $70$  and  $100$  MeV/c. The total systematic uncertainty in the neutron structure function extracted was  $8.7\%$  [27], with an overall  $10\%$  scale uncertainty due to cross normalization of the BONuS data to existing  $F_2^n/F_2^d$  parametrizations.

The kinematic coverage, shown in Fig. 1 (with the  $4.223$  and  $5.262$  GeV data combined), extends from the quasielastic peak to the deep-inelastic region, at  $W^2 \lesssim 5 \text{ GeV}^2$ . The curves in Fig. 1 represent the fixed- $W^2$  thresholds for the four mass regions considered. Typical  $F_2^n$  spectra are shown in Fig. 2 for  $Q^2 = 1.2$  and  $2.4 \text{ GeV}^2$ , with the data restricted to spectator proton angles greater than  $100^\circ$  relative to the momentum transfer, and proton momenta between  $70$  and  $100$  MeV/c. The BONuS results are compared with the ABKM global PDF fit [37] to deep-inelastic and other high-energy scattering data, with inclusion of target mass corrections and higher twist effects. The qualitative agreement between the parametrization and data suggests evidence for quark–hadron duality, which we explore more quantita-

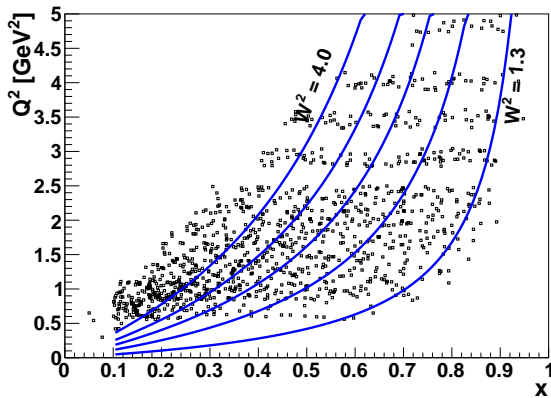


FIG. 1. Kinematic coverage of the BONuS data. The solid lines denote the fixed- $W^2$  thresholds for the four final state mass regions in Eq. (2), from  $W^2 = 1.3$  to  $4.0$   $\text{GeV}^2$ .

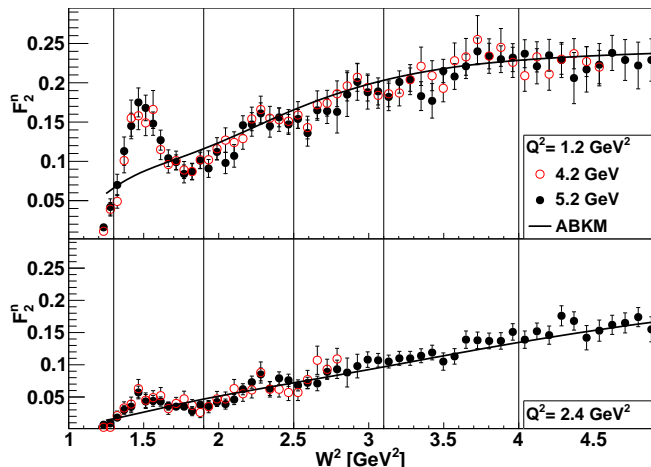


FIG. 2. Representative neutron  $F_2$  structure function spectra from the BONuS experiment at  $Q^2 = 1.2$   $\text{GeV}^2$  (top panel) and  $Q^2 = 2.4$   $\text{GeV}^2$  (bottom panel). The open (filled) circles represent data for a beam energy of  $E = 4.223$  (5.262)  $\text{GeV}$ . The solid curve is computed from the ABKM global PDF parametrization [37] with higher twist effects and target mass corrections.

tively in the following.

### III. TRUNCATED MOMENTS AND LOCAL QUARK-HADRON DUALITY

Because the kinematic variables  $Q^2$ ,  $x$  and  $W^2$  are not independent, a range in  $W^2$  at fixed  $Q^2$  implies a corresponding range in  $x$ . This allows for a straightforward integration of the experimental  $F_2^n$  structure function data to obtain the truncated moments  $M_n$  in Eq. (1). To minimize the model dependence, we evaluate the integrals based solely on the experimentally measured data

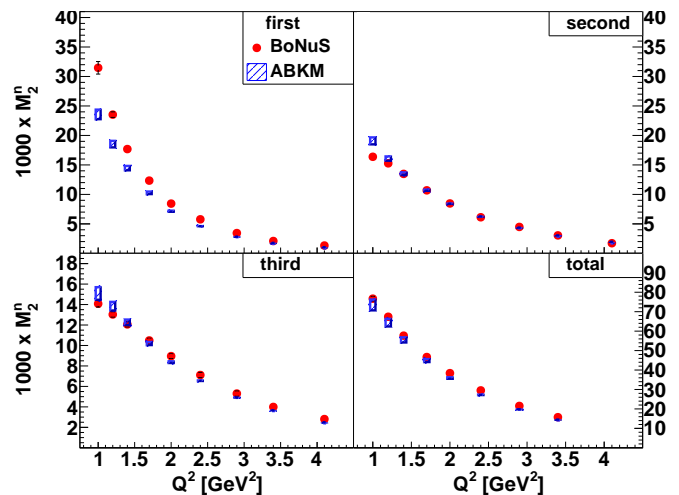


FIG. 3. Second ( $N = 2$ ) neutron truncated moments  $M_2$  for the four resonance regions in Eq. (2) as a function of  $Q^2$ . The moments obtained from the BONuS data (filled circles) are compared with moments computed from the ABKM global PDF parametrization [37] including target mass and higher twist corrections (shaded rectangles).

points, without using any interpolating or extrapolating function.

#### A. Truncated neutron moments

The second ( $N = 2$ ) truncated moments,  $M_2$ , obtained from the BONuS data are shown in Fig. 3 as a function of  $Q^2$  for the four  $W^2$  intervals defined in Eq. (2). The numerical values for the moments are also listed in Table I. The quoted errors take into account the experimental statistical and systematic uncertainties added in quadrature, but do not include the 10% scale uncertainty due to cross normalization of the data. The experimental moments are compared with the moments calculated from the ABKM global PDF parametrization [37], including finite- $Q^2$  corrections from target mass and higher twist effects. The latter are needed in order to obtain a more quantitative description of duality in the low- $Q^2$  region to which the structure functions fitted to the high energy data are extrapolated.

The comparison shows generally very good agreement in the second and third resonance regions, and in the total integrated  $W^2$  interval, while the PDF-based result underestimates the data somewhat in the  $\Delta$  resonance region. The corresponding higher order truncated moments ( $N = 4$  and  $N = 6$ ) are listed in Tables II and III, respectively. Comparison with the ABKM fit (not shown) reveals a similar pattern as for the lowest moment, although the deviation in the lowest- $W$  interval is more pronounced, especially at low  $Q^2$ , because of the greater weighting given to the high- $x$  region in the higher moments.

$Q^2$ [GeV <sup>2</sup> ]	$M_2 [\times 10^{-3}]$			
	1st	2nd	3rd	total
1.0	31.5 ± 1.1	16.4 ± 0.4	14.1 ± 0.3	76.7 ± 1.2
1.2	23.5 ± 0.5	15.3 ± 0.3	13.0 ± 0.3	67.4 ± 0.6
1.4	17.7 ± 0.4	13.5 ± 0.2	12.1 ± 0.3	57.7 ± 0.5
1.7	12.3 ± 0.3	10.7 ± 0.2	10.5 ± 0.2	46.7 ± 0.5
2.0	8.4 ± 0.2	8.5 ± 0.2	9.0 ± 0.2	38.4 ± 0.4
2.4	5.8 ± 0.2	6.1 ± 0.1	7.1 ± 0.3	29.5 ± 0.4
2.9	3.4 ± 0.1	4.5 ± 0.1	5.3 ± 0.3	21.5 ± 0.4
3.4	2.1 ± 0.1	3.1 ± 0.1	4.0 ± 0.2	15.8 ± 0.3
4.1	1.3 ± 0.1	1.7 ± 0.1	2.8 ± 0.1	—

TABLE I. Second ( $N = 2$ ) truncated moments (in units of  $10^{-3}$ ) of the neutron  $F_2$  structure function from the BONuS data for the  $W^2$  regions in Eq. (2). The errors are a quadrature sum of statistical and systematic uncertainties, but do not include the overall 10% normalization uncertainty.

$Q^2$ [GeV <sup>2</sup> ]	$M_4 [\times 10^{-3}]$			
	1st	2nd	3rd	total
1.0	11.58 ± 0.43	3.09 ± 0.08	1.69 ± 0.04	17.49 ± 0.44
1.2	9.80 ± 0.21	3.51 ± 0.06	1.95 ± 0.04	16.78 ± 0.22
1.4	8.11 ± 0.17	3.60 ± 0.06	2.17 ± 0.04	15.61 ± 0.19
1.7	6.27 ± 0.14	3.40 ± 0.06	2.33 ± 0.05	14.01 ± 0.17
2.0	4.67 ± 0.14	3.08 ± 0.06	2.36 ± 0.06	12.45 ± 0.17
2.4	3.48 ± 0.11	2.54 ± 0.06	2.20 ± 0.08	10.59 ± 0.15
2.9	2.22 ± 0.10	2.11 ± 0.07	1.93 ± 0.09	8.52 ± 0.16
3.4	1.44 ± 0.09	1.58 ± 0.07	1.64 ± 0.08	6.72 ± 0.15
4.1	0.95 ± 0.08	0.98 ± 0.07	1.29 ± 0.06	—

TABLE II. As in Table I, but for the  $N = 4$  moment.

Note that while early phenomenological analyses of quark–hadron duality typically compared resonance region data at low  $Q^2$  with scaling functions extrapolated from fits to high- $W$  cross sections [5, 6], subsequent, more quantitative analyses [8, 18] have emphasized the need to take into account the  $Q^2$  dependence in the high- $W$  data, including both leading and higher twist contributions. This is especially important in the high- $x$  region, where the separation between the leading and higher twists is more model dependent due to the absence of high- $Q^2$  measurements, and comparison of resonance region data with the total extrapolated structure functions reveals an enhanced persistence of duality down to lower values of  $Q^2$ .

To study the systematics of local quark–hadron duality

$Q^2$ [GeV <sup>2</sup> ]	$M_6 [\times 10^{-3}]$			
	1st	2nd	3rd	total
1.0	4.39 ± 0.18	0.60 ± 0.01	0.20 ± 0.01	5.28 ± 0.18
1.2	4.19 ± 0.10	0.82 ± 0.01	0.30 ± 0.01	5.45 ± 0.10
1.4	3.79 ± 0.09	0.98 ± 0.02	0.39 ± 0.01	5.38 ± 0.09
1.7	3.24 ± 0.08	1.09 ± 0.02	0.52 ± 0.01	5.17 ± 0.08
2.0	2.62 ± 0.08	1.13 ± 0.02	0.62 ± 0.02	4.82 ± 0.09
2.4	2.12 ± 0.07	1.06 ± 0.02	0.68 ± 0.02	4.41 ± 0.08
2.9	1.45 ± 0.07	1.00 ± 0.03	0.71 ± 0.03	3.77 ± 0.08
3.4	0.99 ± 0.07	0.82 ± 0.04	0.67 ± 0.03	3.14 ± 0.09
4.1	0.68 ± 0.06	0.56 ± 0.04	0.60 ± 0.03	—

TABLE III. As in Table I, but for the  $N = 6$  moment.

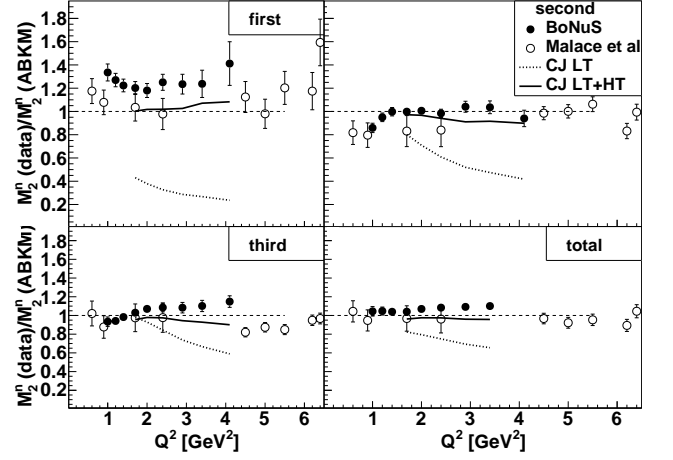


FIG. 4. Ratios of truncated moments of the neutron  $F_2$  structure function from the BONuS data to those computed from the ABKM global PDF parametrization [37] including finite- $Q^2$  effects (filled circles) as a function of  $Q^2$  for the four  $W^2$  intervals in Eq. (2). The empirical moments are compared with the results of the model-dependent analysis of inclusive DIS data [18] (open circles), and with ratios computed from the CJ12 distributions [38], with leading twist only (dotted lines) and including finite- $Q^2$  effects (solid lines). All ratios are taken relative to the ABKM moments.

in more detail, we form ratios of the truncated moments of  $F_2^n$  obtained from the BONuS data to the moments computed from the ABKM reference structure function [37], over the same range of  $x$ . The ratios for the  $M_2$  moments are shown in Fig. 4 as a function of  $Q^2$  for the four invariant mass regions in Eq. (2). The ratios for the second, third and total resonance regions are close to unity, to within  $\sim 10\%$  over the entire range of  $Q^2 = 1$ –4 GeV<sup>2</sup>, and exhibit weak scale dependence. This points to a dramatic confirmation of the validity of local duality for the neutron in these regions. In the first resonance region, the  $\Delta$  resonance is  $\sim 20$ –30% larger than the PDF-based fit, but still displays a similar  $Q^2$  behavior. This could be interpreted as either a stronger violation of local duality in the  $\Delta$  region, which may be expected at lower  $W$ , or possibly underestimated strength of the ABKM parametrization in the large- $x$  regime, to which this  $W$  region corresponds.

The confirmation of the approximate validity of duality in  $F_2^n$  from the BONuS data disfavors the suggestion [17] that duality occurs in the proton because of accidental cancellations of quark charges associated with higher twist, four-quark operators, and disagrees with the prediction that duality should therefore not be seen in the neutron. This conclusion was also reached in the model-dependent analysis by Malace *et al.* [18], who studied duality in the neutron by extracting the  $F_2^n$  structure function from inclusive DIS data using phenomenological deuteron wave functions and an iterative deconvolution procedure [24]. Overall, the BONuS data are in good agreement with the earlier results [18], within the experi-

mental uncertainties, although they appear to lie systematically higher in the  $\Delta$  region. This may be associated with the nuclear corrections in the deuteron, which are subject to greater uncertainties at the largest  $x$  (smallest  $W$ ) values, or a systematic bias of the subtraction method in relation to the various theoretical assumptions and models [19].

The relevance of the finite- $Q^2$  corrections is illustrated in Fig. 4, where the experimental and computed ABKM truncated moments are also compared with the moments calculated from the CTEQ-Jefferson Lab (CJ) global PDF parametrization [38] (from the CJ12min and CJ12max fits [39]) with and without the addition of higher twist corrections. While the ratio of the moments computed from the ABKM and CJ fits is close to unity over the entire range of  $Q^2$  considered when finite- $Q^2$  effects are taken into account, the deviation from unity of the ratio computed from only the leading twist components of the CJ fit can be up to  $\sim 30$ –40% for the integrated resonance region, and up to twice as much for the  $\Delta$  region. This suggests an important role played by the finite- $Q^2$  corrections to the scaling functions in realizing the cancellations between the individual resonance regions that are required for the realization of quark-hadron duality [40–42]. The explicit inclusion of higher twist terms in these parametrization allows for extending the region of validity into the large- $x$  domain. The interplay between higher twist and target mass corrections and their influence on leading twist PDFs at large  $x$  was studied in detail in Ref. [43].

## B. Isospin dependence

The stronger violation of local duality in the  $\Delta$  region is also evident in the ratio of neutron to proton truncated moments, shown in Fig. 5 compared with the reference ABKM parametrization [37]. In order to minimize the systematic uncertainties in the duality comparisons, the proton moments here have been constructed from the same ABKM global fit for the high- $W$  region and the parametrization of the resonance region from Ref. [44]. (Duality in the proton structure function moments themselves was studied in detail in a number previous analyses [7, 8], and generally confirmed at the 10–15% level for the  $N = 2$  moment when integrated over the entire resonance region.)

The significant duality violation in the neutron/proton ratio observed in the  $\Delta$  region can be understood from the isovector nature of the  $\Delta$ -isobar and the relatively small nonresonant background on which it sits. In the limit of exact isospin symmetry, the transitions from a ground state nucleon to an isospin-3/2 resonance would be identical for protons and neutrons. Nonresonant background and isospin symmetry breaking contributions would give rise to differences between proton and neutron moments, but these are typically very small in the  $\Delta$  region. In contrast, the proton and neutron deep-

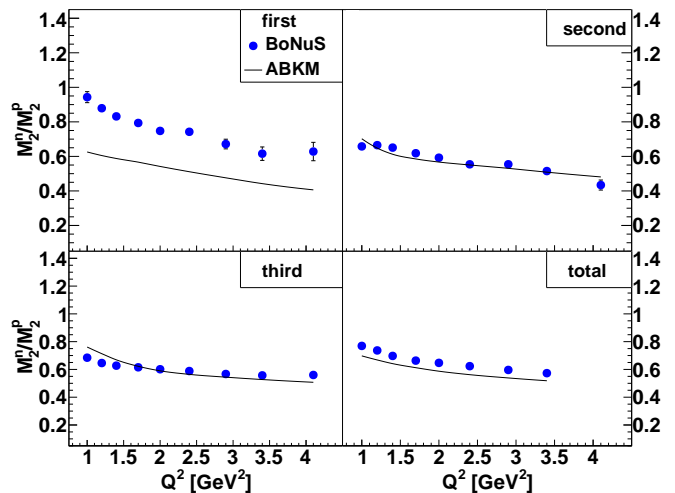


FIG. 5. Ratios  $M_2^n/M_2^p$  of neutron to proton truncated moments of the  $F_2$  structure function versus  $Q^2$ , for the four  $W$  regions in Eq. (2). The BONuS results (filled circles) are compared with the moments computed from the ABKM global PDF parametrization including TMCs and higher twists (solid lines). In both cases the proton moments are evaluated from the same ABKM fit [37].

inelastic structure functions (either leading twist only or with higher twist corrections) in the  $\Delta$  region are expected to be quite different, since at large  $x$  the neutron structure function is strongly suppressed relative to the proton,  $F_2^n \ll F_2^p$  [45, 46]. Thus the fact that the experimental  $M_2^n/M_2^p$  ratio in the  $\Delta$  region lies somewhat higher than the DIS parametrization (even more pronounced than in Ref. [18]), as well as the ratios in the higher- $W$  intervals, is consistent with the duality expectations.

A similar comparison of the neutron to proton moments in the second and third resonance regions in Fig. 5 shows significantly better agreement with the DIS parametrization. The expectation from simple quark models, based on the dominance of magnetic couplings, is for the resonance contributions to the neutron moments to underestimate the DIS function in the second resonance region due to the small couplings to octet spin-1/2 states, while the proton moments would overestimate the DIS results in the second and third regions [41, 42, 47]. While there was some evidence for such a pattern from the earlier, model-dependent analysis of inclusive data [18], there is no indication from the BONuS results of a suppression in the second resonance region. The slightly larger overall magnitude of the neutron moments compared with Ref. [18] brings the present results into almost perfect agreement with the DIS moments in the second region, with a small enhancement in the third region. The corresponding enhancement of the proton data in the third resonance region relative to the ABKM fit [7, 8] then results in essentially no deviation of the neutron to proton ratio here, as illustrated in Fig. 5. Fi-

nally, for the total integrated region between threshold and  $W = 2$  GeV, the empirical  $M_2^n/M_2^p$  ratio is slightly above the DIS result mostly because of the large enhancement of the data in the  $\Delta$  region.

#### IV. CONCLUSION

In this work we have investigated local quark-hadron duality in the neutron structure function based on data from the BONuS experiment at Jefferson Lab [26, 27], which used a novel experimental technique to create an effective neutron target by tagging low momentum spectator protons in electron-deuteron scattering. The spectator tagging technique provides smaller systematic uncertainties compared with the traditional method of subtracting smeared hydrogen data and from inclusive deuteron structure functions, assuming a specific model for the nuclear corrections.

We have evaluated the  $N = 2, 4$  and  $6$  truncated moments of the neutron  $F_2^n$  structure function for the three standard nucleon resonance regions and the total integrated resonance region up to  $W = 2$  GeV, over the range  $Q^2 = 1.0$  to  $4.1$  GeV<sup>2</sup>. Comparison of the experimental moments with moments computed from global parametrizations of PDFs fitted to deep-inelastic and other high energy scattering data, as well as with the corresponding truncated moments for the proton, reveals a dramatic confirmation of local duality for the neutron in the second, third and total resonance regions to better than 10% for the lowest moment. The stronger ( $\sim 20$ –30%) violation of duality in the  $\Delta$  region is consistent with the expectations based on isospin symmetry for the isovector transition amplitudes and the behavior of the  $F_2^n/F_2^p$  ratio at large  $x$  [38, 46].

The confirmation of local duality in the neutron disfavors the model [17] in which duality in the proton arises through accidental cancellations of quark charges associated with higher twist, four-quark operators, which would predict strong duality violations in the neutron. Rather, it suggests a dynamical origin of duality in which

cancellations among nucleon resonances produce a higher degree of duality over the entire resonance region, with stronger violations locally [41, 42, 47]. On the other hand, detailed comparisons between the empirical truncated moments and DIS parametrizations in the individual resonance regions suggest a pattern of duality violation that is more involved than that predicted by simple spin-flavor symmetric quark models with magnetic coupling dominance.

Our results also confirm and refine the findings of earlier model-dependent studies [18] of duality in the neutron in which the neutron structure was extracted from inclusive proton and deuteron data assuming a model for the nuclear corrections and an iterative deconvolution procedure [24]. In particular, the BONuS moments are found lie slightly higher than the earlier results, especially in the  $\Delta$  region, but with a similar  $Q^2$  dependence.

In the future, the spectator tagging technique will be used at Jefferson Lab with an 11 GeV electron beam to extend the kinematical coverage of  $F_2^n$  measurements to higher values of  $x$  and  $Q^2$  [48]. As well as providing more stringent constraints on the leading twist PDFs in the limit  $x \rightarrow 1$ , the new data will allow more definitive tests of local quark-hadron duality for the neutron over a greater range of  $Q^2$ .

#### ACKNOWLEDGMENTS

This work was supported by the DOE Contract No. DE-AC05-06OR23177, under which Jefferson Science Associates, LLC operates Jefferson Lab. The JMU group was supported by the National Science Foundation (NSF) under Grant No. PHY-1307196. S.K. acknowledges the support from the United States Department of Energy (DOE) under grant DE-FG02-96ER40960. J.A. acknowledges the support from the United States Department of Energy (DOE) under grant DE-AC02-06CH11357. S.T. acknowledges the support from the United States Department of Energy (DOE) under grant DE-FG02-97ER41025.

- 
- [1] P. Jimenez-Delgado, W. Melnitchouk and J. F. Owens, J. Phys. G: Nucl. Part. Phys. **40**, 093102 (2013).
  - [2] S. Forte and G. Watt, Ann. Rev. Nucl. Part. Sci. **63**, 291 (2013).
  - [3] A. DeRujula, H. Georgi and H. D. Politzer, Ann. Phys. **103**, 315 (1975).
  - [4] K. G. Wilson, Phys. Rev. **179**, 1499 (1969).
  - [5] E. D. Bloom and F. G. Gilman, Phys. Rev. Lett. **25**, 1140 (1970).
  - [6] E. D. Bloom and F. G. Gilman, Phys. Rev. D **4**, 2901 (1971).
  - [7] I. Niculescu *et al.*, Phys. Rev. Lett. **85**, 1186 (2000).
  - [8] S. P. Malace *et al.*, Phys. Rev. C **80**, 035207 (2009).
  - [9] N. Bianchi, A. Fantoni and S. Liuti, Phys. Rev. D **69**, 014505 (2004).
  - [10] W. Melnitchouk, R. Ent and C. E. Keppel, Phys. Rep. **406**, 127 (2005).
  - [11] P. Monaghan, A. Accardi, M. E. Christy, C. E. Keppel, W. Melnitchouk and L. Zhu, Phys. Rev. Lett. **110**, 152002 (2013).
  - [12] I. Niculescu, J. Arrington, R. Ent and C. E. Keppel, Phys. Rev. C **73**, 045206 (2006).
  - [13] A. Airapetian *et al.*, Phys. Rev. Lett. **90**, 092002 (2003).
  - [14] P. Bosted *et al.*, Phys. Rev. C **75**, 035203 (2007).
  - [15] P. Solvignon *et al.*, Phys. Rev. Lett. **101**, 182502 (2008).
  - [16] S. P. Malace, W. Melnitchouk and A. Psaker, Phys. Rev. C **83**, 035203 (2011).

- [17] S. J. Brodsky, arXiv:hep-ph/0006310.
- [18] S. P. Malace, Y. Kahn, W. Melnitchouk and C. E. Keppel, Phys. Rev. Lett. **104**, 102001 (2010).
- [19] J. Arrington, J. G. Rubin and W. Melnitchouk, Phys. Rev. Lett. **108**, 252001 (2012).
- [20] M. Osipenko, W. Melnitchouk, S. Simula, S. Kulagin and G. Ricco, Nucl. Phys. **A766**, 142 (2006).
- [21] L. B. Weinstein, E. Piasetzky, D. W. Higinbotham, J. Gomez, O. Hen and R. Shneor, Phys. Rev. Lett. **106**, 052301, (2011).
- [22] O. Hen, A. Accardi, W. Melnitchouk and E. Piasetzky, Phys. Rev. D **84**, 117501 (2011).
- [23] O. Hen, E. Piasetzky, L. B. Weinstein and D. W. Higinbotham, Phys. Rev. C **85**, 047301 (2012).
- [24] Y. Kahn, W. Melnitchouk and S. A. Kulagin, Phys. Rev. C **79**, 035205 (2009).
- [25] H. Fenker *et al.*, Nucl. Instr. Meth. A **592**, 273 (2008).
- [26] N. Baillie *et al.*, Phys. Rev. Lett. **108**, 199902 (2012).
- [27] S. Tkachenko *et al.*, Phys. Rev. C **89**, 045206 (2014).
- [28] S. Forte and L. Magnea, Phys. Lett. B **448**, 295 (1999).
- [29] S. Forte, L. Magnea, A. Piccione and G. Ridolfi, Nucl. Phys. **B594**, 46 (2001).
- [30] A. Piccione, Phys. Lett. B **518**, 207 (2001).
- [31] D. Kotlorz and A. Kotlorz, Phys. Lett. B **644**, 284 (2007).
- [32] A. Psaker, W. Melnitchouk, M. E. Christy and C. E. Keppel, Phys. Rev. C **78** 025206 (2008).
- [33] B. A. Mecking *et al.*, Nucl. Instr. Meth. A **503**, 513 (2003).
- [34] C. Ciofi degli Atti, L.P. Kaptari and B.Z. Kopeliovich, Eur. Phys. J. A **19**, 133 (2004).
- [35] W. Cosyn and M. Sargsian, Phys. Rev. C **84**, 014601 (2011).
- [36] W. Cosyn, W. Melnitchouk and M. Sargsian, Phys. Rev. C **89**, 014612 (2014).
- [37] S. Alekhin, J. Blumlein, S. Klein and S. Moch, Phys. Rev. D **81** 014032 (2010).
- [38] J. F. Owens, W. Melnitchouk and A. Accardi, Phys. Rev. D **87**, 094012 (2013).
- [39] <http://www.jlab.org/cj>.
- [40] N. Isgur, S. Jeschonnek, W. Melnitchouk and J. W. Van Orden, Phys. Rev. D **64**, 054005 (2001).
- [41] F. E. Close and N. Isgur, Phys. Lett. B **509**, 81 (2001).
- [42] F. E. Close and W. Melnitchouk, Phys. Rev. C **68**, 035210 (2003).
- [43] A. Accardi *et al.*, Phys. Rev. D **81** 034016 (2010)
- [44] M. E. Christy and P. E. Bosted, Phys. Rev. C **81**, 055213 (2010).
- [45] F. E. Close and A. W. Thomas, Phys. Lett. B **212**, 227 (1988).
- [46] W. Melnitchouk and A. W. Thomas, Phys. Lett. B **377**, 11 (1996).
- [47] F. E. Close and W. Melnitchouk, Phys. Rev. C **79**, 055202 (2009).
- [48] Jefferson Lab Experiment E12-10-102, S. Bültmann, M. E. Christy, H. Fenker, K. Griffioen, C. E. Keppel, S. Kuhn and W. Melnitchouk, spokespersons.